PROCEEDINGS OF SCIENCE

Geant4-aided Quantum State Selective Decay Spectroscopy of ^{213}Ra

Christian Lorenz*, **Luis G. Sarmiento and Dirk Rudolph**
Department of Physics, Lund University, S-22100 Lund, Sweden
E-mail: Christian.Lorenz@nuclear.lu.se

Michael Block
GSI Helmholtzzentrum für Schwerionenforschung, D-64291 Darmstadt, Germany

Utilizing the excellent mass resolving power of SHIPTRAP and the charged-particle-γ multi-coincidence setup TASISpec, the decay path of the ^{213}Ra ground state can be exclusively studied. Based on virtual experiments with Geant4 it is possible to refine the α-branching ratios of the ^{213}Ra ground state as well as γ-ray branching ratios in the ^{209}Rn daughter. The present study provides a proof of concept where clean quantum-state selective particle-γ decay spectroscopy is used in conjunction with detailed Geant4 Monte-Carlo simulations to gain insight into nuclear structure properties.

PACS: 23.20.-g 23.60.+e 27.80.+w

The 26th International Nuclear Physics Conference
11-16 September, 2016
Adelaide, Australia

*Speaker.

PoS(INPC2016)073

1. Introduction

State of the art simulation toolkits for particle and nuclear physics have been proven to be a more and more used and valued resource for planning, analyzing, and interpreting experimental data. The most frequently used and developed toolkits are Geant4 [1], FLUCA [2], and MCNP [3]. They are continuously under development and reach a very high level of accuracy and performance. In nuclear physics simulations are widely used to study detector responses and efficiencies. In this work we are using Geant4 to perform detailed virtual experiments which are then confronted with the results of a real experiment. If the properties of the detector and all experimental conditions are well understood, any remaining inconsistencies must arise from incorrect physics input, i.e. incorrect decay schemes. By manipulating the latter and self-consistently checking the outcome against the results of the experiment, one gains information about the relevant physics parameters and can deduce new or revised values for various types of decay data.

Nuclei far from the line of β stability receive increasing attention in contemporary nuclear structure studies. Particularly challenging are heavy and superheavy elements. Here, fusion-evaporation reactions are the exclusive way to produce isotopes of interest. Due to rather small cross-sections (μb to pb) those nuclei are hidden in a cocktail of other reaction products and it is nearly impossible to prepare an isotopically clean source with any kind of standard recoil spectrometers. A rather novel method of preparing such an isotopically clean beam is to select the desired ground or isomeric state of the nucleus in question with a Penning trap. After the purification in the Penning trap the selected nuclei are transferred to a high-resolution particle-γ coincidence setup and studied further. This experimental scheme is exceptionally suited to be confronted with virtual experiments as described before because of the basically non-existent background.
Such an experiment was realized at GSI Darmstadt using the TASISpec detector system [4] placed behind SHIPTRAP [5] to study the decay path of the ^{213}Ra ground state, detailed in section 2 [6].

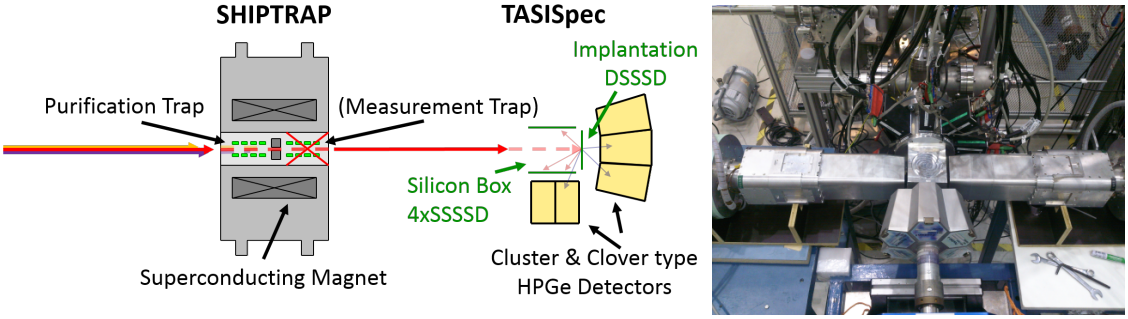

(a) (b)

Figure 1: (a) Schematic view of the experimental setup. The beam is coming from the left and the desired quantum state is selected by the purification trap. After implantation in the DSSSD their decay can be studied with the decay station TASISpec. (b) The TASISpec setup behind JYFLTRAP for studying the weak proton decay branch of $^{53}Co^{m}$ [7]. Here the beam is coming from the top and 2 clover detectors were employed instead of 1.

In figure 1a the experimental scheme is depicted. The TASISpec decay station consisted of five silicon strip detectors arranged in a cube: four single-sided silicon strip detectors (SSSSD, 1.0-mm thick, 16 stripes) referred to as 'box detectors' and one double-sided silicon strip detector (DSSSD, 0.31-mm thick, $32 \times 32 = 1024$ pixels) facing the beam direction - the 'implantation detector'. Due to the low kinetic energy of ≈ 3 keV after being extracted from the trap, the ^{213}Ra ions were rather deposited on the dead-layer surface than actually implanted in active silicon-detector material. In addition to the silicon box, one former EUROBALL CLUSTER detector [8] placed behind the DSSSD, and one VEGA CLOVER detector [9] placed behind one of the SSSSDs were employed for γ and X-ray detection. This setup allows for detailed decay studies using particle-photon coincidences. The whole TASISpec setup has been implemented and simulated in detail with Geant4 [10].

All together - the TASISpec decay station, its virtual representation in Geant4 and a 100% pure beam from SHIPTRAP - provide the necessary ingredients to perform 'Geant4-aided quantum state selective decay spectroscopy'.

2. The ^{213}Ra decay path

Studying the decay path of ^{213}Ra gives insight into the shell structure of nuclei in the proximity of the classic neutron shell closure at $N = 126$. The majority of the known α and electron-capture (EC) branching ratios of ^{213}Ra [11, 12] and its decay daughters [13, 14, 15, 16] have been measured in the 1960s and remained basically unchanged until present [17, 18]. More recent studies focus primarily on the α decay of ^{213}Ra to the low-lying states in ^{209}Rn [19, 20], partially relying on the α-decay branching ratios into the ground and first excited states of ^{209}Rn from the early ^{213}Ra studies. Figure 2 comprises the evaluated branching ratios and nuclear properties relevant for this study.

The most prominent features in the particle spectrum are the α-peaks from ^{213}Ra decay to the ground and first excited state of ^{209}Rn, and the α-peaks from the ^{213}Fr, ^{209}Rn and ^{209}At decays (see. figure 3a). Detector signals were only recorded if they stem from one of the silicon detectors (threshold ~ 500 keV for the present experiment) or if silicon and germanium (threshold ~ 30 keV) detectors were in coincidence. Therefore, all γ and X-ray peaks in the photon spectrum shown in figure 3b originate only from transitions in ^{209}Rn.

The mass-resolving power of SHIPTRAP's purification trap is readily sufficient to separate the ^{213}Ra ground state from other reaction products as well as its $17/2^-$ isomeric state at 1770 keV. This ensures that all features in the detected spectra have their origin in the decay of the ^{213}Ra ground state and its daughter nuclei. Furthermore, it avoids the necessity of assumptions about background contributions as they were necessary to e.g. determine the α/EC branching ratio of ^{213}Ra in ref. [11]. The experimental data was recorded in listmode events during 15 h with a trap-release frequency of 2.5/s.

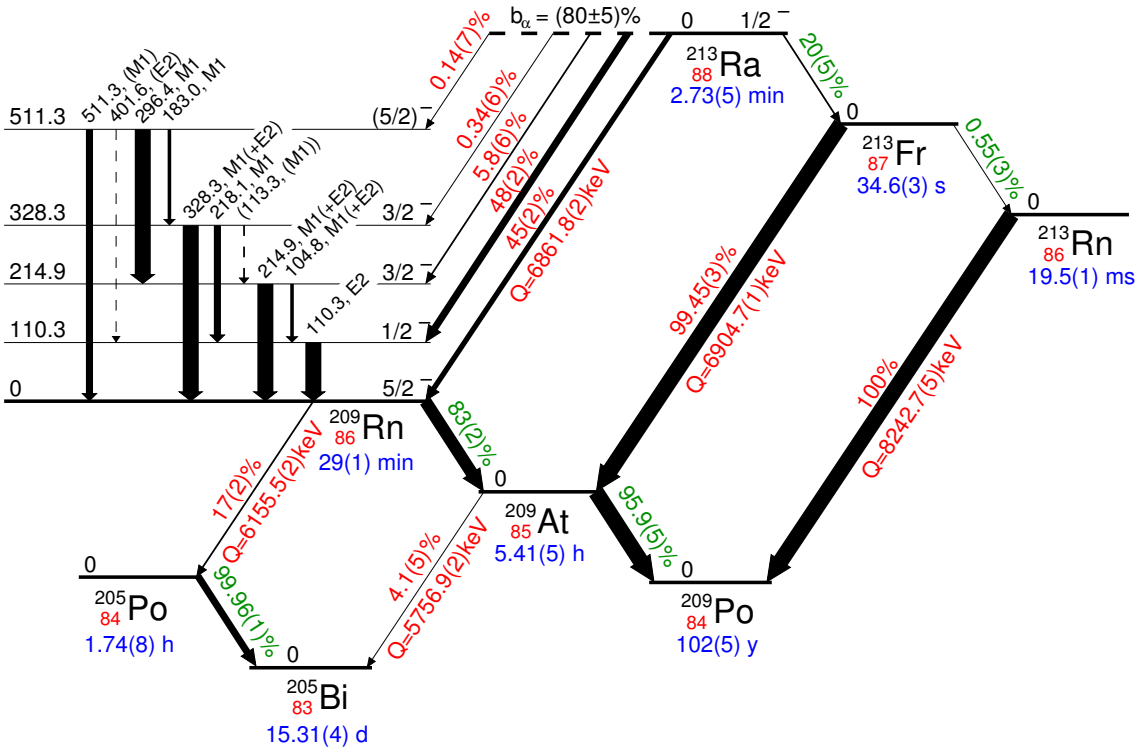

Figure 2: The hitherto known decay properties relevant for the ^{213}Ra ground-state decay path [18, 22, 23].

3. Virtual Geant4-Experiment

To simulate the entire experiment the evaluated implementation of TASISpec in Geant4 [10] has been configured to precisely match the experimental conditions of the present case study. $^{213}Ra^{2+}$ ions were generated at a rate of 2.5/s and virtually implanted into the dead-layer of the implantation DSSSD resembling the experimental beam spot. As in the real experiment, only events detected within the 15 h experiment duration are stored for further analysis, imitating the accumulation of radioactivity from the ^{213}Ra decay.

The only unknown parameter concerning the experimental setup is the dead-layer thickness of the silicon detectors. For similar types of DSSSDs the dead layer is known to be in the order of 2 μm [21]. To account for that uncertainty all virtual experiments have been repeated with different dead-layer thicknesses. The simulated data is then given as input to the exact same analysis code as for the experimental data. Furthermore each simulation is repeated several times to investigate statistical fluctuations and significance of parameters that are used to compare simulation and experiment.

Due to the very shallow implantation of the ions into the dead layer, the detected α-particle energy is strongly affected by the path length through the dead layer, depending on the emission angle. Obviously, different dead-layer thicknesses affect the detected α-particle energy as well. Therefore, each simulation with a different simulated dead-layer thickness must be recalibrated with respect to the experiment.

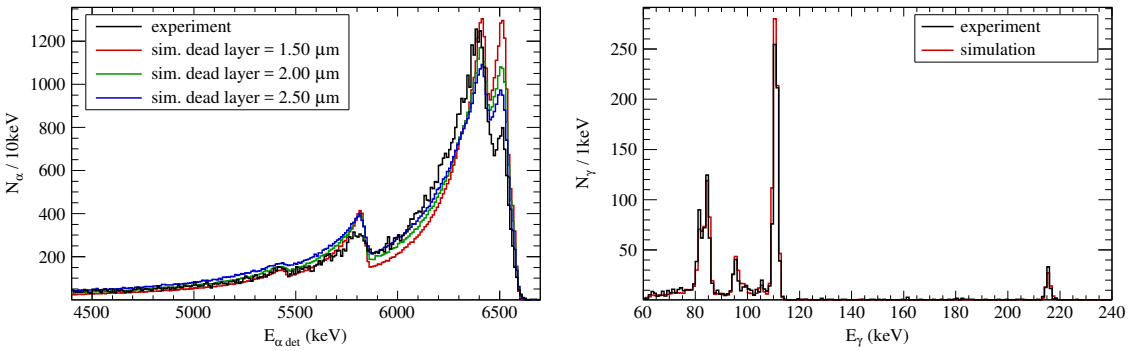

(a) (b)

Figure 3: Comparison between simulation and experiment using evaluated data: (a) the particle spectrum varying the dead-layer of the implantation detector and (b) the normalized γ-ray spectrum.

Besides all experimental parameters related to the setup, Geant4 requires the input of radioactive decay data and the decay schemes of the involved nuclei comprising α and γ branching ratios, multipolarities, and mixing ratios.

Using evaluated data [18, 22, 23] the experimentally observed α-spectrum cannot be reproduced, even if the dead-layer thickness is strongly varied. This is illustrated in figure 3a. For thicker dead layers, the left tail of the α-peaks becomes more pronounced because the α-particles have to pass through more material before they reach the active detector volume. Furthermore, the yield in the photon spectrum is nearly a factor of two too low in the simulation. This suggests that α-decay branching ratios to the excited states of ^{209}Rn are underestimated. On the other hand, comparing the normalized simulated photon spectrum with the experiment indicates that the relative feeding of those states, their γ-branchings and assigned multipolarities fit rather well (see figure 3b).

The overestimated peak to the very right in the spectra of figure 3a comprises two contributions: *(i)* the ^{213}Fr α-decay, the yield of which is primarily determined by the α/EC branching ratio of ^{213}Ra, and *(ii)* the ^{213}Ra ground-state to ground-state α-decay into ^{209}Rn. Adjusting their branchings until best agreement is achieved already leads to a significant improvement in the α-spectrum while enhancing the yield in the photon spectrum. To determine the branching ratios that result in the best agreement, each simulation with a different branching ratio is compared to the experiment by means of a χ^2-test. The first step of this procedure is shown in figure 4a. There the total α-branching ratio of ^{213}Ra is varied and a minimum χ^2 at $b_\alpha = 87$ % is found. Having that value fixed, the ^{213}Ra ground-state to ground-state α-branching ratio is varied and the value with the smallest χ^2 is calculated and fixed. This sequence is repeated until the respective values with the smallest χ^2 do not change. The resulting values for the two adjusted branchings remain unchanged during subsequent iterations. Another case exemplifying the use of the χ^2-test is shown in figure 4b. Here the relative α-branching ratio of the ^{213}Ra ground-state decay into the first excited state of ^{209}Rn is varied. One can see that the χ^2-value of the α-spectrum as well as γ-spectrum has a minimum at ~ 66 % .

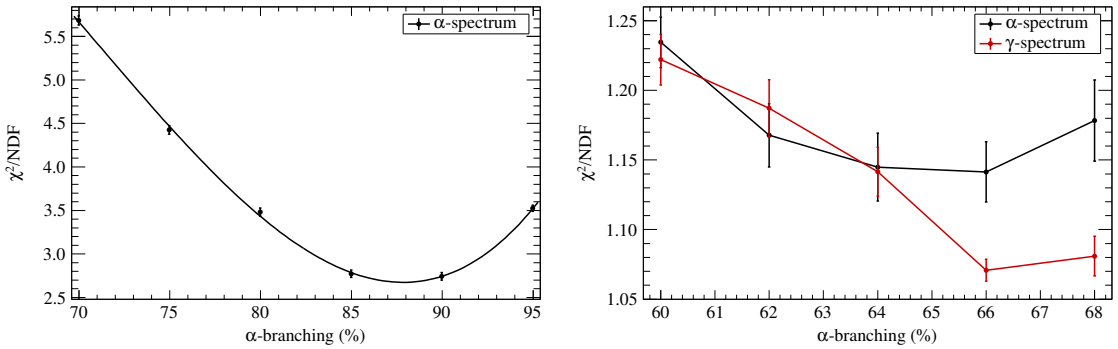

(a) (b)

Figure 4: (a) The first step of adjusting the total α-branching ratio of the ^{213}Ra ground-state decay. A minimum χ^2 value is found at 87 % and is fixed for the next iteration. (b) The dependency of the χ^2 value on the α-branching ratio of ^{213}Ra ground-state decay into the first excited state of ^{209}Rn, after the total ^{213}Ra α-branching ratio and the relative α-branching ratio to the ^{209}Rn ground state have been adjusted.

The shape of the α-spectrum between 6.0 and 6.4 MeV is only determined by the ^{213}Ra α-decay to the excited states of ^{209}Rn. Investigating their relative branchings is very difficult when relying on the particle spectrum only. Since the de-excitation of ^{209}Rn is the only origin of γ and X-rays, the photon and α-photon coincidence spectra can be used *jointly* to study the transitions in ^{209}Rn and the feeding pattern into the corresponding states. Relevant coincidence spectra are the particle spectra in prompt coincidence with X-rays, the 110 keV γ-ray transition in ^{209}Rn, and the particle spectra in prompt coincidence with any photon. The particle spectrum in prompt coincidence with the 215 keV γ-ray transition has very low statistics and is therefore of minor relevance. These coincidence spectra can be compared between simulation and experiment by spectrum shape and yield.

To find out which parameter (e.g., α and γ-ray branching ratios or multipolarity) to adjust in order to improve on one of the mentioned criteria without impairing on another is a very complex task, because all parameters involved are highly correlated. For example, changing the relative γ-ray branchings of the second excited state in ^{209}Rn has not only impact on the respective γ-ray peaks in the photon spectrum. It also alters the X-ray yield, the intensity of the 110 keV transition, and the yields and shapes of the corresponding α-photon coincidence spectra.

After many iterations of manipulating α and γ-ray branching ratios, and multipolarities, it was found that the discrepancies between simulation and experiment can be resolved by simply modifying the relative α-branching ratios into the excited states of ^{209}Rn. The hitherto reported decay scheme of ^{209}Rn as such can be confirmed. In particular it is possible to conclude that the 215 keV and 105 keV γ-ray transition are rather pure $M1$ than mixed $E2/M1$ transitions.

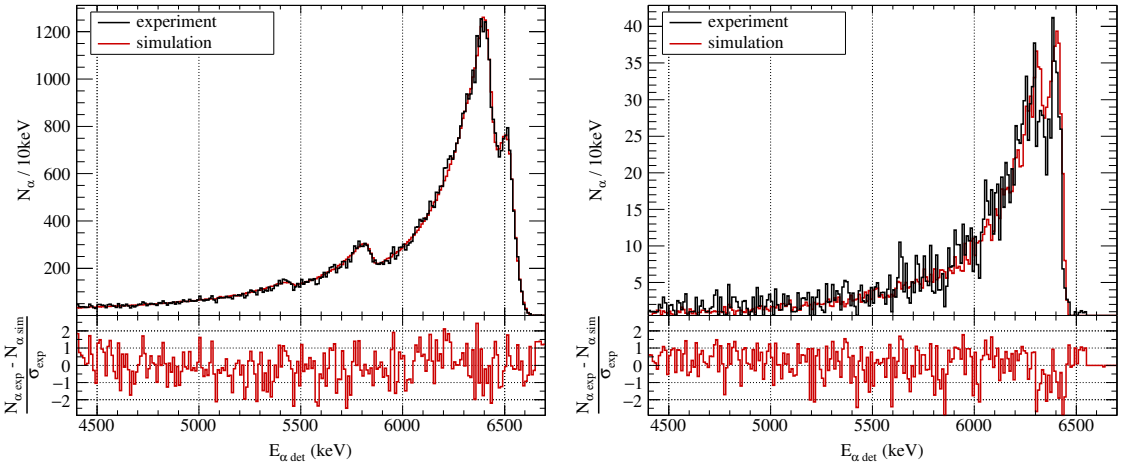

Figure 5: Comparison between the final simulation and experiment: (a) the particle spectrum of the implantation detector and (b) the particle-photon coincidence spectrum.

Finally, the remaining discrepancies between virtual and real experiment in the α-spectrum below 6 MeV (see figure 3a) can be addressed by decreasing the α-decay branching ratios of ^{209}At and ^{209}Rn by ~ 40 %. The final spectra of the simulation are shown in figure 5 and are in excellent agreement with the experimentally observed spectra [24].

It is important to note that the recoil energies from α-decays are large compared to the implantation energy. Therefore, when an α-particle is detected in the DSSSD, the recoiling nucleus most likely escaped the detector volume. In case of the ^{213}Ra α-decay the impact on the α-photon coincidences is expected to be negligible since the transitions in ^{209}Rn are prompt. This effect becomes more important for determining the ^{209}Rn and ^{209}At α/EC branching ratios because of their rather long half-lives (28.8 min and 5.42 h respectively). Effects which are not reassembled in the simulation e.g. vacuum pumps could bias the results in that case and might explain the lower α-branching in ^{209}At and ^{209}Rn we observe.

While conducting this study, the effect of different beam energies, i.e. implantation depth of the ^{213}Ra ions, has been investigated. Simulations for beam energies between 1 keV and 5 keV with SRIM [25] result in implantation depth ranging from ~ 40 to 80 Å. Therefore, one expects no significant changes in the simulated spectra because (*i*) the implantation depth is orders of magnitudes smaller than the ~ 2 μm dead-layer and (*ii*) the recoil energies from α-decays are in the order of 110 keV, much higher than the implantation energy. Surprisingly, changing the beam energy from 2.5 to 3.0 keV in Geant4 leads to significantly different results. It appears that for a ≥ 3.0 keV beam Geant4 overestimates backscattering so that 'implanted' ^{213}Ra ions are scattered out of the detector volume again. This primarily results in much lower yields in all spectra, which does not match experimental observation. Therefore, the study was conducted with a 2.5 keV beam in Geant4, which should be of no significant importance according to SRIM and leads to a

consistent picture. This issue has been found in the Geant4 version 10.1 as well as in the currently latest version 10.3.

4. Conclusion

Using the example of the ^{213}Ra ground-state decay, the procedure of how to determine decay data using quantum state selective decay spectroscopy in combination with state of the art Monte Carlo simulations has been discussed. It proves to be a valuable technique for reviewing /improving older decay data and to gain insight into nuclear structure properties of nuclei far from line of β stability, where cross-sections are very small.
Of special relevance is, that this setup provides a background free measurement. This allows for studies of nuclei whose decay patterns are not separable from decay patterns of beam contaminants. One example is the decay of the isomeric and the ground state of ^{53}Co [7].
A framework for automatizing and optimizing the described procedure is under development.

Acknowledgments

This work is supported by the Swedish Research Council (VR 2011-5253 and VR 2013-4271), the Knut and Alice Wallenberg Foundation (KAW 2015.0021), the Royal Physiographic Society in Lund, and the German Federal Ministry of Education and Research (BMBF).

References

[1] S. Agostinelli *et al.*, Nucl. Instr. Meth. A **506**, 250 (2003).

[2] T.T. Böhlen *et al.*, Nucl. Data Sheets **120**, 211 (2014).

[3] T. Goorley *et al.*, Nuclear Technology **180**, 298 (2012).

[4] L.-L. Andersson *et al.*, Nucl. Instr. Meth. A **622**, 164 (2010).

[5] M. Block *et al.*, Eur. Phys. J. D **45**, 39 (2007).

[6] D. Rudolph *et al.*, GSI Scientific Report **2009**, 177 (2010).

[7] L.G. Sarmiento *et al.*, (to be published).

[8] J. Eberth *et al.*, Nucl. Instr. Meth. A **369**, 135 (1996).

[9] J. Gerl, H. Grawe, E. Roeckl, and H.J. Wollersheim, GSI Darmstadt, Report, 1998.

[10] L.G. Sarmiento, L.-L. Andersson, and D. Rudolph, Nucl. Instr. Meth. A **667**, 26 (2012).

[11] K. Valli, W. Treytl, and Earl K. Hyde, Phys. Rev. **161**, 1284 (1967).

[12] Y.V. Lobanov, and V.A. Durin, Soviet J. Nucl. Phys. **8**, 493 (1969).

[13] R.D. Griffioen, and R.D. MacFarlane, Phys. Rev. **133**, B1373 (1964).

[14] N.A. Golovkov, S. Guetkh, B.S. Dzhelepov, Y.V. Norseev, V.A. Khalkin, and V.G.Chumin, Bull. Acad. Sci. USSR, Phys. Ser. **33**, 1489 (1970).

[15] N.A. Golovkov, R.B. Ivanov, A. Kolaczkowski, Y.V. Norseev, and V.G. Chumin, Bull. Acad. Sci. USSR, Phys. Ser. **35**, 2063 (1972).

[16] P. Hornshoy, P.G. Hansen, and B. Jonson, Nucl. Phys. **A230**, 380 (1974).

[17] A. Rytz, Atomic Data Nucl. Data Tables **47**, 205 (1991).

[18] J. Chen, and F.G. Kondev, Nucl. Data Sheets **126**, 373 (2015).

[19] F.P. Heßberger, S. Hofmann, I. Kojouharov, and D. Ackermann, Eur. Phys. J. A **22**, 253 (2004).

[20] P. Kuusiniemi, F.P. Heßberger, D. Ackermann, S. Antalic, S. Hofmann, K. Nishio, B. Sulignano, I. Kojouharov, and R. Mann, Eur. Phys. J. A **30**, 551 (2006).

[21] U. Forsberg *et al.*, Eur. Phys. J. **66**, 02036 (2014).

[22] M.S. Basunia, Nucl. Data Sheets **108**, 633 (2007).

[23] F.G. Kondev, Nucl. Data Sheets **101**, 521 (2004).

[24] Ch. Lorenz *et al.*, (to be published).

[25] J.F. Ziegler, M.D. Ziegler, J.P. Biersack, Nucl. Instr. Meth. B **268**, 1818 (2010).